SUPPLEMENTAL INFORMATION

Details on Transformer

In Figure S1, a schematic is given for the step up transformer and the connections to the tandem IMS drift tube. Not shown in this graphic are ion shutter control electronics and the detector amplifier since emphasis is given to the transformer here. A photograph of the transformer is given in Figure S2.

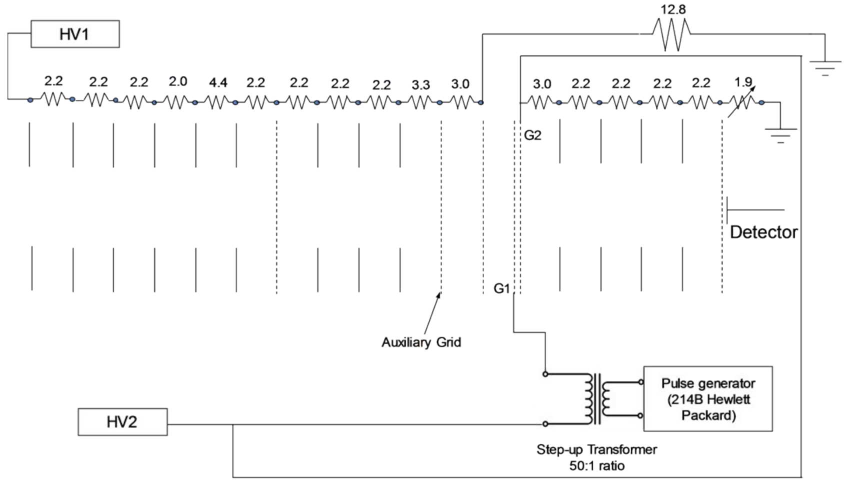

Figure S1. The tandem ion mobility spectrometry with three wire grid assembly. The auxiliary grid is the distance of 0.3 cm from grid 1 and the distance between grid 1 and grid 2 is 0.65 mm. Ferrite, model no 3F4 is used in the transformer with one turn on the primary wire and 50 turns on the secondary wire providing 50 X gain on waveform amplitude. Potentials on drift rings from the ion source region (at left) to the Auxiliary Grid is controlled by a High Voltage Supply (HV1) and a voltage divider with discrete resistors as shown (units of MOhm). Grid 1 is provided the RF waveform on a DC component, established by a second high voltage supply (HV2) which also drives potentials on Grid 2 and remaining drift rings.

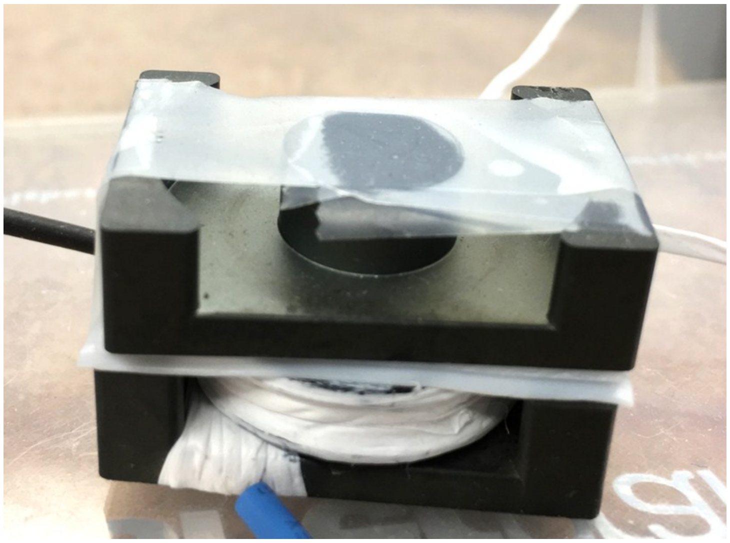

Figure S2. Photograph of in-house built transformer. The primary and secondary windings around the ferrite core are retained using a length of ordinary laboratory grade Teflon tape. A second ferrite core is used with Teflon sheet insulation only to add mechanical strength to the small transformer.

Comment
The Identity of Interferents A and B will be disclosed upon request and review.

In-house Build Amplifier
The amplifier gain was constant at 5 x 10^{10} V/amp and was generated using an in-house amplifier with design shown below in Figure S3.

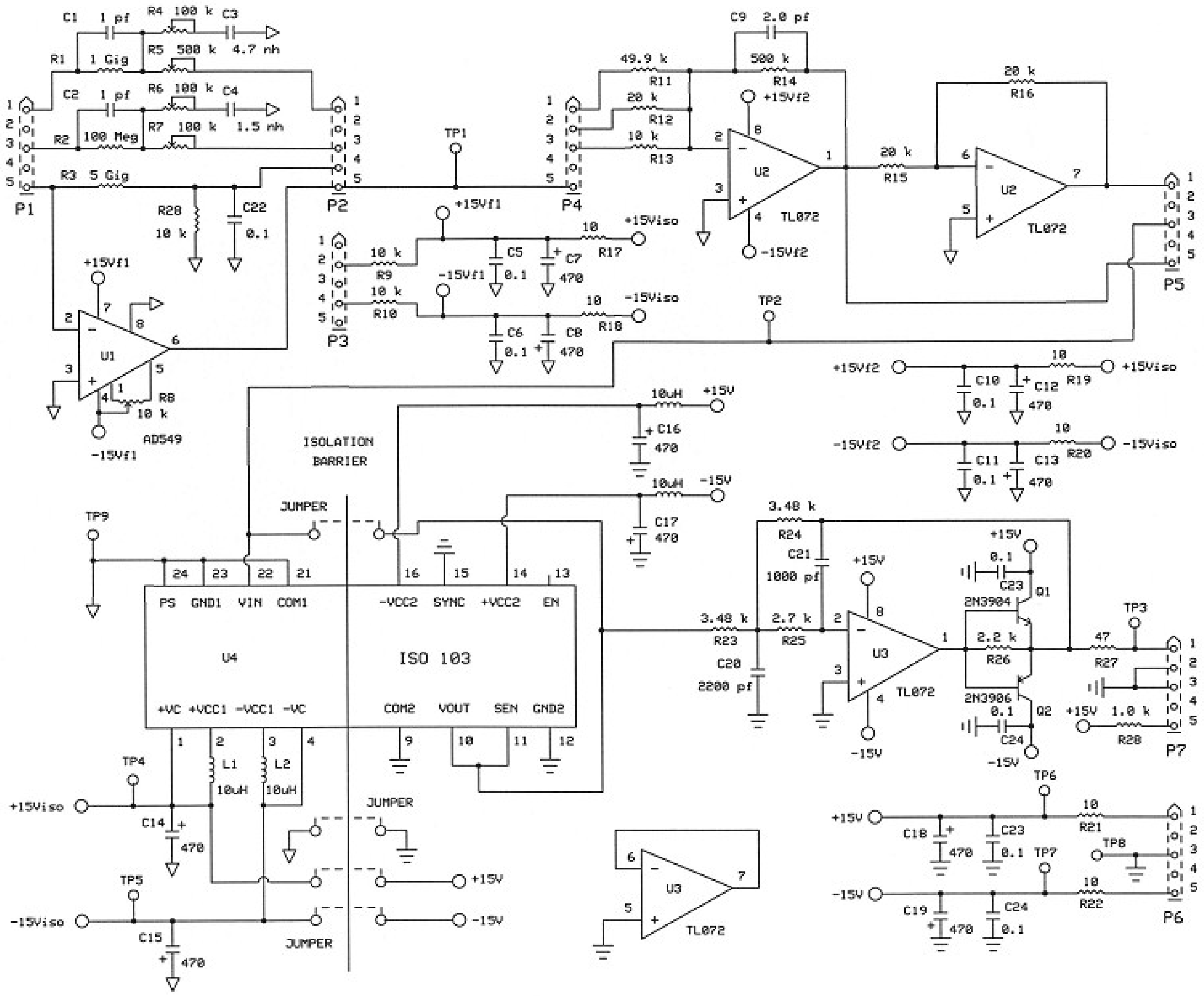

Figure S3. Amplifier designed at NMSU by John Carr.

Synchronization of Thermal Desorption of Interferent and Explosive
In this research grade tandem IMS analyzer, the thermal desorber was connected to the ionization volume of the drift tube by a length of ceramic tubing which exhibited gas solid chromatographic behavior which was unwelcome and would not be seen in a commercial ETD. Consequently, “retention times” for explosives and interferents differed and coordination was necessary to deliver each into the ionization volume when each was at maximum vapor concentration. Differences in retention in the ceramic tube are shown in Figure S4. Consequently, the interferent was desorbed on an ETD based

sample trap and 9 seconds later a separation sample trap containing TNT was thermally desorbed. This procedure provided no benefit for the measurements and complicated procedures slightly.

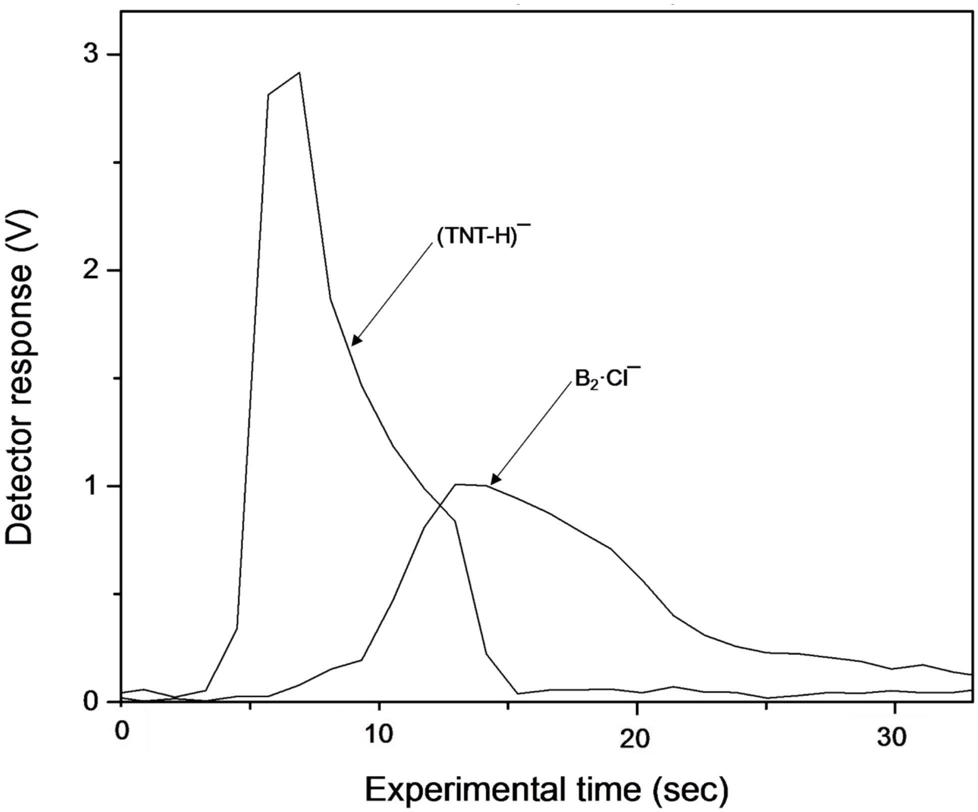

Figure S4. Plots of response following insertion of a sample trap into the thermal desorber inlet of the tandem IMS analyzer.

Relationship between Gas Temperature, Field Strength and Ion Energy for the Decomposition of PETN·Cl^- in the Wire Grid Assembly

Results in Figure S5 are plots of Percent Fragmentation vs. Electric Field (Td) at Four Temperatures constructed from data in Figure 4 and are intended to show an association between ion heating from the electric field and from gas temperature. An ion can be heated by thermal, field and collision sources and the first two terms dominate in a strong electric field. As temperature is increased, the field needed for fragmentation decreases and an equivalence has been proposed between E (Td) and gas temperature (°C).

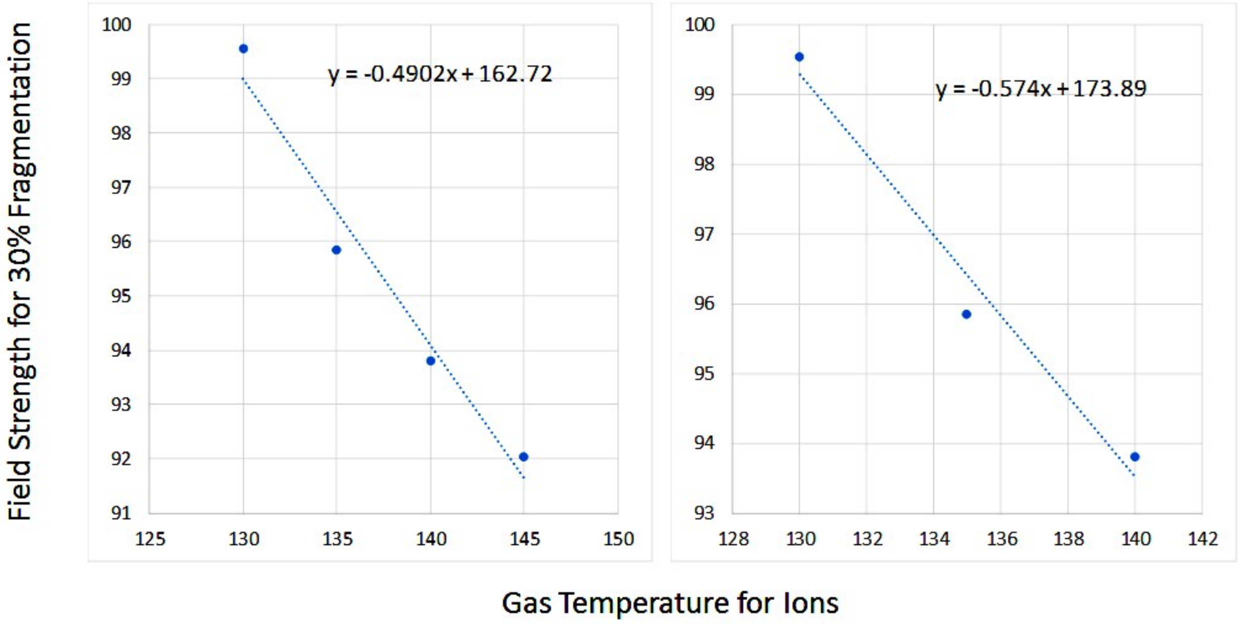

Figure S5. Plots extracted from Figure 4 at 30% Fragmentation to obtain a correlation between field strength and gas temperature of ions. Two plots are shown here for the field strength for 30% fragmentation and regression is made for four temperatures (left) yielding a relationship of 0.49 Td/˚C. A plot with only the three higher temperatures (right) shows a slope of 0.57 Td/˚C with full appreciation of the limitations of such a plot.

Previous determinations of the equivalence of energy (thermal vs. E/N) were made with a comparatively simple structure provided in a planar DMS analyzer. The complex wire grid assembly used in this manuscript was more complex and included ion energies over a yet unknown though large distribution.

Influence of Energy of Activation for Decomposition of Chloride Adducts of Explosives

The curves in Figure S6 describe the relationship between changes in energy of activation for ion fragmentation and the Electric Field Strength in the wire grid assembly. As with Figure S5, these plots are based on the additive relationship between thermal and field sources and the energy of an ion.

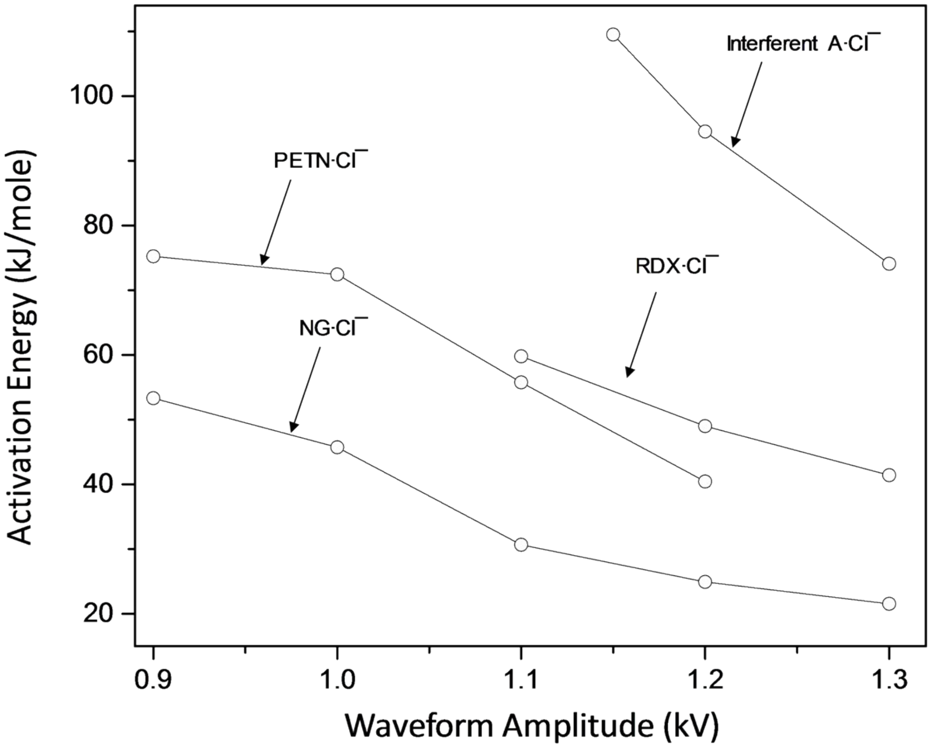

Figure S6. Plots of Activation Energy with Electric Field Strength determined from fragmentation of gas ions of explosives and Interferent B.

Differences in the slopes of these plots and relative placement can be attributed to substance, that is, ion structure and composition. These patterns suggest additional controls in the determination of explosives using tandem IMS with a reactive stage. Although Interferent B has large activation energies compared to those for the substitution reactions of these explosives, the steep slope suggests effective promotion of decomposition over a narrow range of field energy. This was observed with the near complete removal of Interferent B from TNT.

Note that TNT is not included in this plot since field decomposition of $(TNT\text{-}1)^-$ was not observed under conditions employed in this study.